

Received 4 April 2022
Accepted 13 June 2022

Edited by W. T. A. Harrison, University of Aberdeen, Scotland

Keywords: tellurium; pyrazine; heterocyclic; supramolecular; crystal structure.

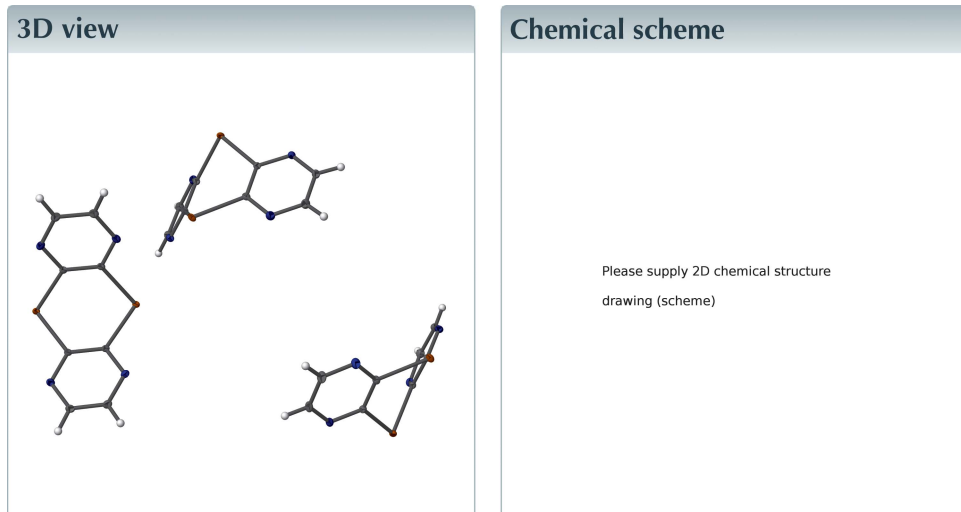
Structural data: full structural data are available from iucrdata.iucr.org

[1,4]Ditellurino[2,3-*b*:5,6-*b'*]dipyrazine

Donna Franklin,^a Aundrea Lee,^a Frank R. Fronczek^b and Thomas Junk^{a*}

^aDepartment of Chemistry, Lafayette, LA 70403, USA, and ^bDepartment of Chemistry, Louisiana State University, Baton Rouge, LA 70803, USA. *Correspondence e-mail: thomas.junk@louisiana.edu

[1,4]Ditellurino[2,3-*b*:5,6-*b'*]dipyrazine represents the first reported [1,4]chalcogeno[2,3-*b*:5,6-*b'*]dipyrazine containing a heavy chalcogens. The asymmetric unit consists of three molecules. In contrast to its sulfur analog, which is planar [Lynch *et al.* (1994) *J. Cryst. Struct. Commun.* **50**, 1470–1472], C₈H₄N₄Te₂ is folded along the Te···Te axis to accommodate the larger chalcogenide atoms. The dihedral angle between the two Te₂C₂ rings of the central ring is 57.9° (mean of three). C–Te bond lengths range from 2.1105 (16) Å to 2.1381 (17) Å, in good agreement with those predicted by their covalent radii. All Te atoms are involved in intermolecular Te···N contacts, with distances in the range 2.894 (2) to 2.963 (2) Å. These result in a spiral supramolecular assembly, forming helical columns.



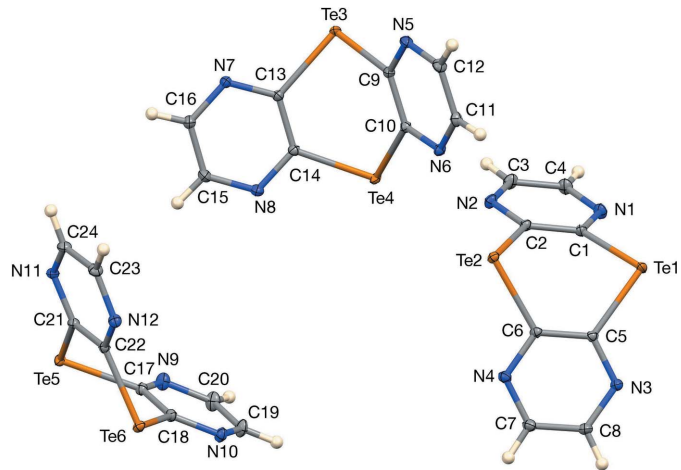
Structure description

Heterocyclic tellurium compounds have found considerable attention due to their tendency to form supramolecular assemblies including molecular wires (Kremer *et al.*, 2016), ribbons (Cozzolino *et al.*, 2010) and rings (Ho *et al.*, 2016, 2017). Such assemblies can give rise to materials with non-linear optical properties (Cozzolino *et al.*, 2010), as well as novel phosphorescent organic emitters (Kremer *et al.*, 2015). A ribbon motif resulting from secondary intermolecular N···Te bonding interactions of 2.767 (6) and 2.659 (6) Å was reported for 3,4-dicyano-1,2,5-telluradiazole (Cozzolino *et al.*, 2010). Similarly, molecular wire motifs resulting from secondary intermolecular N···Te bonding were observed for 2-substituted benzo-1,3-tellurazoles, but with significantly longer N···Te distances. This is exemplified by 2-(2-furanyl) benzo-1,3-tellurazole, 3.17 Å (Kremer *et al.*, 2016) and 1,3-benzotellurazol-2-ylacetonitrile, 3.16 Å (Sanford *et al.*, 2017). Not all Te, N-containing heterocycles form supramolecular wires or ribbons. Thus, 10*H*-pyrazino[2,3-*b*][1,4]benzotellurazine (Smith *et al.*, 2020), 2*H*-1,4-benzo-tellurazin-3(4*H*)-one and 2,3-dihydro-1,5-benzotellurazepin-4(5*H*)-one (Myers *et al.*, 2016) lack this



OPEN ACCESS

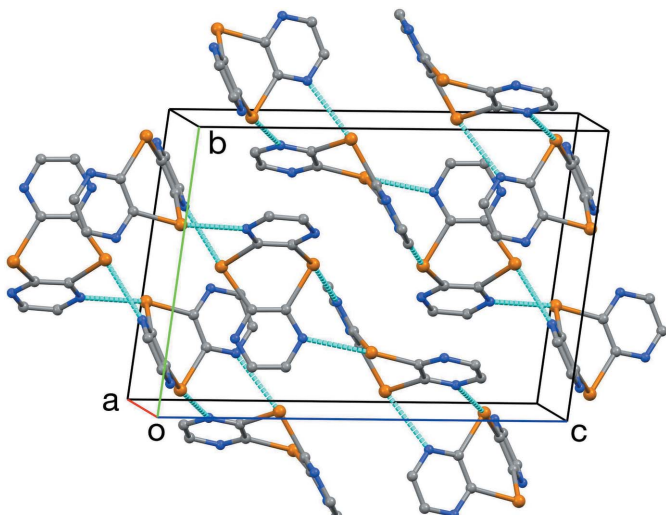
Published under a CC BY 4.0 licence

**Figure 1**

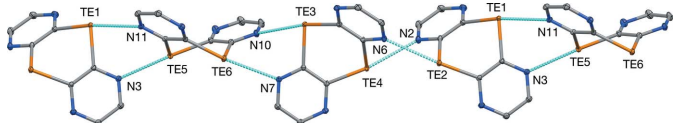
The asymmetric unit of [1,4]ditellurino[2,3-b:5,6-b']dipyrazine with 50% ellipsoids.

feature. The [1,4]dichalcogena[2,3-b:5,6-b']dipyrazines remain poorly explored and no examples containing heavy chalcogens were reported prior to this study.

The three molecules of the asymmetric unit are shown in Fig. 1, which illustrates their folded V shapes. The degree of folding along the Te \cdots Te line can be described by φ , the dihedral angle between the two C_2Te_2 moieties of the central ring. This dihedral angle has a value of $60.08(5)^\circ$ for the molecule containing Te1 and Te2, $57.16(5)^\circ$ for the Te3/Te4 molecule, and $56.54(5)^\circ$ for the Te5/Te6 molecule, with a mean value of 57.9° . A sulfur analog of the title compound has been structurally characterized (Lynch *et al.*, 1994), but is planar rather than folded along the chalcogen–chalcogen axis. The corresponding selenium congener remains unreported. The shape of the title compound shows structural similarity to those of 9,10-dichalcogenanthracenes containing tellurium and one other chalcogen atom in the central ring (Dereu *et al.*, 1981; Meyers *et al.*, 1988), as well as to the recently characterized $10H$ -pyrazino[2,3-b][1,4]benzotellurazine (Smith *et*

**Figure 2**

The unit cell, showing intermolecular Te \cdots N contacts.

**Figure 3**

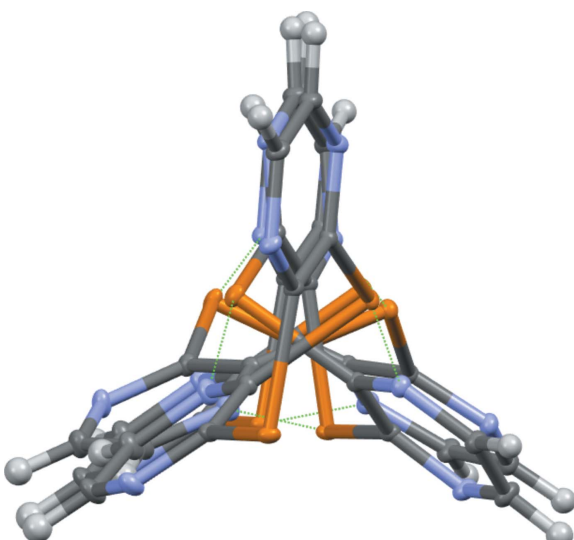
A portion of the helical chain, side view.

al., 2020). All are V-shaped, but the extent to which the center ring is folded varies considerably. The title compound and telluranthrene ($\varphi = 57.86^\circ$) are nearly identical in this respect, while analogous compounds containing nitrogen as one apex heteroatom show much a less pronounced V shape. This is exemplified by dibenzo[b,e]tellurazine, with $\varphi = 18.28^\circ$ (Junk *et al.*, 1993) and $10H$ -pyrazino[2,3-b][1,4]benzotellurazine, $\varphi = 18.29^\circ$ (Smith *et al.*, 2020) for the central C_2TeN moieties.

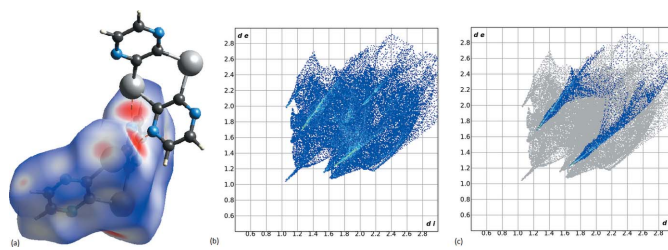
The C–Te–C angles for the three independent molecules of the title compound range from $91.48(6)$ to $93.80(6)^\circ$, similar to those of 95.3 and 95.9° , respectively, previously reported for telluranthrene (Dereu *et al.*, 1981). C–Te bond lengths range from $2.1105(16)$ Å to $2.1381(17)$ Å, in good agreement with those predicted by their covalent radii.

Intermolecular features are dominated by Te \cdots N interactions involving all Te atoms, as shown in Fig. 2. The range of distances for these contacts is $2.894(2)$ to $2.963(2)$ Å. These fall between those of $2.767(6)$ and $2.659(6)$ Å reported for 3,4-dicyano-1,2,5-telluradiazole (Cozzolino *et al.*, 2010) and those for benzo-1,3-tellurazoles, ranging from 2.985 Å for 2-(methylsulfanyl)-1,3-benzotellurazole (Ali *et al.*, 2016) to 3.169 Å for 2-(2-furyl)-1,3-benzotellurazole (Kremer *et al.*, 2016). In contrast, despite its structural similarity, $10H$ -pyrazino[2,3-b][1,4]benzotellurazine does not exhibit any supramolecular Te \cdots N bonding but forms hydrogen-bonded dimers instead (Smith *et al.*, 2020).

Each molecule of the title compound is involved in four Te \cdots N contacts, forming helical chains, as shown in Figs. 3 and 4. The helices have approximate threefold helical symmetry,

**Figure 4**

View of chain along the helix axis.

**Figure 5**

(a) Hirshfeld surface mapped over d_{norm} , (b) two-dimensional fingerprint plot, (c) two-dimensional fingerprint plot with reciprocal $\text{N}\cdots\text{Te}$ contacts highlighted.

with a three-molecule repeat period. The helical chains are in the $[1\bar{1}1]$ direction and have a repeat distance of $20.244(2)$ Å.

The Hirshfeld surface enclosing the Te3/Te4 molecule was calculated with respect to d_e , d_i and d_{norm} using *Crystal Explorer* (Spackman *et al.*, 2021), where d_e and d_i represent the nearest distance of external or internal nucleus from a point of interest on the iso-surface. The dominant $\text{N}\cdots\text{Te}$ interactions with the adjacent Te1/Te2 molecule can be seen as the bright red areas on the Hirshfeld surface. The two-dimensional fingerprint plot and a two-dimensional fingerprint plot highlighting close reciprocal $\text{N}\cdots\text{Te}$ contacts are shown in Fig. 5. These contacts include 14.6% of the surface area.

A search of the Cambridge Structural Database (May 2021 update; Groom *et al.*, 2016) for similar organochalcogen heterocycles yielded 9,10-dichalcogenaanthracenes, $\text{C}_{12}\text{H}_8(X,Y)$, $(X,Y) = (\text{O}, \text{Te})$, (S, Te) , (Se, Te) and (Te, Te) ; PXTELL (Smith *et al.*, 1973), VEHVUZ (Meyers *et al.*, 1988), VEHWEK (Meyers *et al.*, 1988), and BAVJIR (Dereu *et al.*, 1981), respectively. A further comparison was carried out with the sulfur analog of the title compound, WIBWEJ (Lynch *et al.*, 1994), as well as with benzo[1,4]tellurazine derivatives HABJID (Junk *et al.*, 1993), UGIHIEL (Smith *et al.*, 2020) and BUTNOV (Myers *et al.*, 2016). A comparison with other Te, N-containing heterocycles known to undergo supramolecular $\text{Te}\cdots\text{N}$ bonding included 1,3-benzotellurazoles OLUQIX (Kremer *et al.*, 2016), RUVWUC (Kremer *et al.*, 2015), HALWID (Sanford *et al.*, 2017) and 3,4-dicyano-1,2,5-telluradiazole AREGEK01 (Semenov *et al.*, 2012).

Synthesis and crystallization

Preparation of [1,4]ditellurino[2,3-*b*:5,6-*b'*]dipyrazine: a 100 ml round-bottom flask equipped with mechanical stirring and inert gas inlet was charged with tellurium powder (200 mesh, 1.28 g, 10 mmol), sodium hydride (0.6 g of 60% emulsion in mineral oil, 15 mmol) and dry *N*-methyl-2-pyrrolidone (12 ml). The mixture was purged with nitrogen, placed in a Wood's metal bath and heated to 453 K with mechanical stirring for two hours. 2,3-Dichloropyrazine (1.49 g, 10 mmol) was then added, followed by continued stirring at 453 K. The mixture was allowed to cool and diluted with water (100 ml). Solids were collected by filtration and dried. They were subsequently extracted with 2×10 ml of chloroform. The combined extracts were chromatographed on a 1.5×10 cm

Table 1
Experimental details.

Crystal data	$\text{C}_8\text{H}_4\text{N}_4\text{Te}_2$
Chemical formula	411.35
M_r	Triclinic, $P\bar{1}$
Crystal system, space group	90
Temperature (K)	7.6531 (8), 11.7862 (12), 16.8371 (18)
a, b, c (Å)	81.350 (2), 85.884 (2), 80.440 (2)
α, β, γ (°)	1478.9 (3)
V (Å 3)	6
Z	Mo $K\alpha$
Radiation type	5.88
μ (mm $^{-1}$)	0.19 \times 0.17 \times 0.16
Crystal size (mm)	
Data collection	Bruker Kappa APEXII DUO
Diffractometer	CCD
Absorption correction	Multi-scan (<i>SADABS</i> ; Krause <i>et al.</i> , 2015)
T_{\min}, T_{\max}	0.362, 0.453
No. of measured, independent and observed [$I > 2\sigma(I)$] reflections	158610, 158610, 145750
R_{int}	0.025
$(\sin \theta/\lambda)_{\text{max}}$ (Å $^{-1}$)	0.950
Refinement	
$R[F^2 > 2\sigma(F^2)]$, $wR(F^2)$, S	0.024, 0.058, 1.10
No. of reflections	158610
No. of parameters	381
H-atom treatment	H-atom parameters constrained
$\Delta\rho_{\text{max}}, \Delta\rho_{\text{min}}$ (e Å $^{-3}$)	2.18, -0.97

Computer programs: *APEX3* and *SAINT* (Bruker, 2016), *SHELXT2014/5* (Sheldrick, 2015a), *SHELXL2018/1* (Sheldrick, 2015b), *Mercury* (Macrae *et al.*, 2020), and *publCIF* (Westrip, 2010).

column (silica gel, neutral, 200 mesh) using chloroform as mobile phase, followed by chloroform: acetonitrile (10:1 v/v). A yellow band eluted first and was identified as bis(pyrazin-2-yl)tellurium by mass spectrometry. This was followed by a blue band, identified as bis(3-chloropyrazin-2-yl)ditellurium. The following yellow band contained the title compound. Crystallization from chloroform solution furnished yellow crystals, m.p. 413–415 K, yield 46 mg (2.2%).

Properties: ^1H NMR (CDCl_3 , p.p.m.): 8.31 (*s*, 4H). ^{13}C NMR (CDCl_3 , p.p.m.): 1443.46, 154.32. The compound slowly oxidizes when exposed to air in solution. A sample suitable for X-ray crystallography was obtained by evaporation of a solution in chloroform.

Refinement

Crystal data, data collection and structure refinement details are summarized in Table 1. In the later stages of refinement, a small amount of twinning was detected, by 180° rotation about the reciprocal 110 direction. Final refinement was as a twin-component twin using an *HKL5* file prepared by *ROTAX* (Parsons *et al.*, 2003). The BASF parameter is 0.0250 (4).

Acknowledgements

We are grateful to the Department of Chemistry, University of Louisiana at Lafayette for material support of this work.

data reports

Funding information

Funding for this research was provided by: Louisiana Board of Regents (grant No. LEQSF(2011-12)-ENH-TR-01).

References

- Ali, A. M. M., Ramazanova, P. A., Abakarov, G. M., Tarakanova, A. V. & Anisimov, A. V. (2016). *CSD Communication* (CCDC 1506868). CCDC, Cambridge, England.
- Bruker (2016). *APEX2* and *SAINT*, Bruker AXS Inc., Madison, Wisconsin, USA.
- Cozzolino, A. F., Yang, Q. & Vargas-Baca, I. (2010). *Cryst. Growth Des.* **10**, 959–964.
- Dereu, N. L. M., Zingaro, R. A. & Meyers, E. A. (1981). *Cryst. Struct. Commun.* **10**, 1359–1364.
- Groom, C. R., Bruno, I. J., Lightfoot, M. P. & Ward, S. C. (2016). *Acta Cryst. B72*, 171–179.
- Ho, P. C., Rafique, J., Lee, J., Lee, L. M., Jenkins, H. A., Britten, J. F., Braga, A. L. & Vargas-Baca, I. (2017). *Dalton Trans.* **46**, 6570–6579.
- Ho, P. C., Szydlowski, P., Sinclair, J., Elder, P. J. W., Kübel, J., Gendy, C., Lee, L. M., Jenkins, H., Britten, J. F., Morim, D. R. & Vargas-Baca, I. (2016). *Nat. Commun.* **7**, 11299.
- Junk, T., Irgolic, K. J., Reibenspies, J. H. & Meyers, E. A. (1993). *Acta Cryst. C49*, 938–940.
- Krause, L., Herbst-Irmer, R., Sheldrick, G. M. & Stalke, D. (2015). *J. Appl. Cryst.* **48**, 3–10.
- Kremer, A., Aurisicchio, C., De Leo, F., Ventura, B., Wouters, J., Armaroli, N., Barbieri, A. & Bonifazi, D. (2015). *Chem. Eur. J.* **21**, 15377–15387.
- Kremer, A., Fermi, A., Biot, N., Wouters, J. & Bonifazi, D. (2016). *Chem. Eur. J.* **22**, 5665–5675.
- Lynch, V. M., Simonsen, S. H., Davis, B. E., Martin, G. E., Musmar, M. J., Lam, W. & Smith, K. (1994). *Acta Cryst. C50*, 1470–1472.
- Macrae, C. F., Sovago, I., Cottrell, S. J., Galek, P. T. A., McCabe, P., Pidcock, E., Platings, M., Shields, G. P., Stevens, J. S., Towler, M. & Wood, P. A. (2020). *J. Appl. Cryst.* **53**, 226–235.
- Meyers, E. A., Irgolic, K. J., Zingaro, R. A., Junk, T., Chakravorty, R., Dereu, N. L. M., French, K. & Pappalardo, G. C. (1988). *Phosphorus Sulfur Relat. Elem.* **38**, 257–269.
- Myers, J. P., Fronczek, F. R. & Junk, T. (2016). *Acta Cryst. C72*, 1–5.
- Parsons, S., Gould, B., Cooper, R. & Farrugia, L. (2003). *ROTAX*. University of Edinburgh, Scotland.
- Sanford, G., Walker, K. E., Fronczek, F. R. & Junk, T. (2017). *J. Heterocycl. Chem.* **54**, 575–579.
- Semenov, N. A., Pushkarevsky, N. A., Beckmann, J., Finke, P., Lork, E., Mews, R., Bagryanskaya, I. Y., Gatilov, Y. V., Konchenko, S. N., Vasiliev, V. G. & Zibarev, A. V. (2012). *Eur. J. Inorg. Chem.* pp. 3693–3703.
- Sheldrick, G. M. (2015a). *Acta Cryst. A71*, 3–8.
- Sheldrick, G. M. (2015b). *Acta Cryst. C71*, 3–8.
- Smith, M. R., Mangion, M. M., Zingaro, R. A. & Meyers, E. A. (1973). *Heteroatom Chem.*, **10**, 527–531.
- Smith, D. S., Alexis, D. N., Fronczek, F. R. & Junk, T. (2020). *Heteroatom Chem.*, article ID 1765950.
- Spackman, P. R., Turner, M. J., McKinnon, J. J., Wolff, S. K., Grimwood, D. J., Jayatilaka, D. & Spackman, M. A. (2021). *J. Appl. Cryst.* **54**, 1006–1011.
- Westrip, S. P. (2010). *J. Appl. Cryst.* **43**, 920–925.

full crystallographic data

IUCrData (2022). **7**, x220622 [https://doi.org/10.1107/S2414314622006228]

[1,4]Ditellurino[2,3-*b*:5,6-*b'*]dipyrazine

Donna Franklin, Aundrea Lee, Frank R. Fronczek and Thomas Junk

[1,4]Ditellurino[2,3-*b*:5,6-*b'*]dipyrazine

Crystal data

$C_8H_{14}N_4Te_2$
 $M_r = 411.35$
Triclinic, $P\bar{1}$
 $a = 7.6531 (8) \text{ \AA}$
 $b = 11.7862 (12) \text{ \AA}$
 $c = 16.8371 (18) \text{ \AA}$
 $\alpha = 81.350 (2)^\circ$
 $\beta = 85.884 (2)^\circ$
 $\gamma = 80.440 (2)^\circ$
 $V = 1478.9 (3) \text{ \AA}^3$

$Z = 6$
 $F(000) = 1104$
 $D_x = 2.771 \text{ Mg m}^{-3}$
Mo $K\alpha$ radiation, $\lambda = 0.71073 \text{ \AA}$
Cell parameters from 9342 reflections
 $\theta = 2.8\text{--}42.1^\circ$
 $\mu = 5.88 \text{ mm}^{-1}$
 $T = 90 \text{ K}$
Fragment, yellow
 $0.19 \times 0.17 \times 0.16 \text{ mm}$

Data collection

Bruker Kappa APEXII DUO CCD
diffractometer
Radiation source: fine-focus sealed tube
TRIUMPH curved graphite monochromator
 φ and ω scans
Absorption correction: multi-scan
(SADABS; Krause *et al.*, 2015)
 $T_{\min} = 0.362$, $T_{\max} = 0.453$

158610 measured reflections
158610 independent reflections
145750 reflections with $I > 2\sigma(I)$
 $R_{\text{int}} = 0.025$
 $\theta_{\max} = 42.5^\circ$, $\theta_{\min} = 1.2^\circ$
 $h = -14\text{--}14$
 $k = -22\text{--}22$
 $l = -31\text{--}31$

Refinement

Refinement on F^2
Least-squares matrix: full
 $R[F^2 > 2\sigma(F^2)] = 0.024$
 $wR(F^2) = 0.058$
 $S = 1.10$
158610 reflections
381 parameters
0 restraints
Primary atom site location: structure-invariant
direct methods
Secondary atom site location: difference Fourier
map

Hydrogen site location: inferred from
neighbouring sites
H-atom parameters constrained
 $w = 1/[\sigma^2(F_o^2) + (0.0009P)^2 + 1.6438P]$
where $P = (F_o^2 + 2F_c^2)/3$
 $(\Delta/\sigma)_{\max} = 0.002$
 $\Delta\rho_{\max} = 2.18 \text{ e \AA}^{-3}$
 $\Delta\rho_{\min} = -0.97 \text{ e \AA}^{-3}$
Extinction correction: SHELXL-2018/1
(Sheldrick 2015b),
 $F_c^* = kFc[1 + 0.001xFc^2\lambda^3/\sin(2\theta)]^{-1/4}$
Extinction coefficient: 0.00036 (7)

Special details

Geometry. All esds (except the esd in the dihedral angle between two l.s. planes) are estimated using the full covariance matrix. The cell esds are taken into account individually in the estimation of esds in distances, angles and torsion angles; correlations between esds in cell parameters are only used when they are defined by crystal symmetry. An approximate (isotropic) treatment of cell esds is used for estimating esds involving l.s. planes.

Refinement. Refined as a two-component twin using an HKL5 file prepared by ROTAX (Parsons *et al.*, 2003). The BASF parameter is 0.0250 (4). All H atoms were located in difference maps and then treated as riding in geometrically idealized positions with C—H distances 0.95 Å and with $U_{\text{iso}}(\text{H}) = 1.2U_{\text{eq}}$ for the attached C atom.

Fractional atomic coordinates and isotropic or equivalent isotropic displacement parameters (Å²)

	<i>x</i>	<i>y</i>	<i>z</i>	$U_{\text{iso}}^*/U_{\text{eq}}$
Te1	0.49841 (2)	0.50998 (2)	0.85722 (2)	0.01013 (2)
Te2	0.50106 (2)	0.49957 (2)	0.63430 (2)	0.00816 (2)
N1	0.4741 (2)	0.75856 (14)	0.79682 (9)	0.0131 (3)
N2	0.4700 (2)	0.75553 (14)	0.63202 (9)	0.0113 (2)
N3	0.8440 (2)	0.35839 (14)	0.83665 (9)	0.0103 (2)
N4	0.8595 (2)	0.37038 (14)	0.66970 (9)	0.0104 (2)
C1	0.4830 (2)	0.65832 (15)	0.76698 (10)	0.0098 (3)
C2	0.4806 (2)	0.65701 (15)	0.68373 (10)	0.0090 (2)
C3	0.4596 (3)	0.85524 (16)	0.66225 (11)	0.0131 (3)
H3	0.450785	0.926470	0.626760	0.016*
C4	0.4615 (3)	0.85661 (17)	0.74470 (11)	0.0139 (3)
H4	0.453565	0.928841	0.764348	0.017*
C5	0.7087 (2)	0.41601 (15)	0.79341 (10)	0.0086 (2)
C6	0.7142 (2)	0.41927 (15)	0.70924 (10)	0.0084 (2)
C7	0.9955 (2)	0.31457 (16)	0.71338 (11)	0.0118 (3)
H7	1.100495	0.280085	0.687036	0.014*
C8	0.9850 (2)	0.30641 (17)	0.79687 (11)	0.0118 (3)
H8	1.080803	0.262596	0.826477	0.014*
Te3	0.02141 (2)	0.96211 (2)	0.37609 (2)	0.00927 (2)
Te4	0.45479 (2)	0.80313 (2)	0.45840 (2)	0.00845 (2)
N5	-0.1035 (2)	0.76067 (14)	0.47346 (9)	0.0109 (2)
N6	0.2130 (2)	0.64559 (13)	0.53966 (9)	0.0094 (2)
N7	0.2250 (2)	0.92573 (13)	0.22221 (8)	0.0094 (2)
N8	0.5463 (2)	0.81350 (15)	0.28562 (9)	0.0116 (2)
C9	0.0482 (2)	0.80356 (15)	0.45639 (10)	0.0087 (2)
C10	0.2078 (2)	0.74554 (15)	0.48943 (9)	0.0084 (2)
C11	0.0613 (2)	0.60249 (16)	0.55555 (10)	0.0111 (3)
H11	0.061189	0.531090	0.590301	0.013*
C12	-0.0961 (2)	0.65951 (17)	0.52251 (11)	0.0120 (3)
H12	-0.201159	0.625984	0.534990	0.014*
C13	0.2442 (2)	0.90429 (15)	0.30184 (10)	0.0085 (2)
C14	0.4045 (2)	0.84565 (15)	0.33377 (10)	0.0088 (2)
C15	0.5256 (2)	0.83823 (18)	0.20617 (11)	0.0134 (3)
H15	0.623674	0.818218	0.170301	0.016*
C16	0.3656 (2)	0.89205 (16)	0.17491 (10)	0.0111 (3)
H16	0.355508	0.905375	0.118238	0.013*

Te5	0.92057 (2)	0.34134 (2)	0.00428 (2)	0.00896 (2)
Te6	0.93205 (2)	0.03850 (2)	0.12002 (2)	0.00860 (2)
N9	0.9987 (2)	0.38464 (15)	0.16384 (9)	0.0133 (3)
N10	1.0234 (2)	0.16105 (14)	0.24945 (9)	0.0118 (2)
N11	0.5643 (2)	0.29991 (14)	-0.02659 (9)	0.0100 (2)
N12	0.5688 (2)	0.08150 (14)	0.06426 (9)	0.0105 (2)
C17	0.9704 (2)	0.29510 (15)	0.12895 (10)	0.0094 (3)
C18	0.9813 (2)	0.18233 (15)	0.17227 (10)	0.0092 (2)
C19	1.0551 (3)	0.25069 (17)	0.28327 (11)	0.0143 (3)
H19	1.087619	0.237944	0.337674	0.017*
C20	1.0417 (3)	0.36185 (18)	0.24084 (11)	0.0155 (3)
H20	1.063593	0.423560	0.267200	0.019*
C21	0.7081 (2)	0.24611 (15)	0.01189 (10)	0.0084 (2)
C22	0.7113 (2)	0.13526 (15)	0.05717 (10)	0.0085 (2)
C23	0.4234 (2)	0.13848 (17)	0.02780 (11)	0.0117 (3)
H23	0.318870	0.103801	0.033307	0.014*
C24	0.4216 (2)	0.24684 (17)	-0.01780 (11)	0.0115 (3)
H24	0.316408	0.284193	-0.043376	0.014*

Atomic displacement parameters (\AA^2)

	U^{11}	U^{22}	U^{33}	U^{12}	U^{13}	U^{23}
Te1	0.01103 (4)	0.00946 (4)	0.00761 (4)	0.00239 (3)	0.00198 (3)	0.00057 (3)
Te2	0.00895 (4)	0.00699 (4)	0.00847 (4)	-0.00041 (3)	-0.00201 (3)	-0.00098 (3)
N1	0.0182 (7)	0.0093 (6)	0.0112 (6)	-0.0003 (5)	0.0013 (5)	-0.0026 (5)
N2	0.0145 (6)	0.0085 (6)	0.0105 (5)	-0.0016 (5)	-0.0021 (5)	0.0004 (4)
N3	0.0089 (5)	0.0111 (6)	0.0099 (5)	0.0000 (5)	-0.0007 (4)	-0.0002 (5)
N4	0.0096 (6)	0.0105 (6)	0.0112 (5)	-0.0001 (5)	-0.0001 (4)	-0.0036 (5)
C1	0.0107 (6)	0.0087 (6)	0.0089 (6)	0.0004 (5)	0.0004 (5)	-0.0005 (5)
C2	0.0096 (6)	0.0075 (6)	0.0094 (6)	-0.0007 (5)	-0.0006 (5)	0.0000 (5)
C3	0.0173 (8)	0.0082 (7)	0.0133 (7)	-0.0022 (6)	-0.0014 (6)	0.0003 (5)
C4	0.0188 (8)	0.0092 (7)	0.0136 (7)	-0.0013 (6)	0.0008 (6)	-0.0026 (5)
C5	0.0081 (6)	0.0078 (6)	0.0093 (6)	-0.0006 (5)	0.0001 (5)	-0.0002 (5)
C6	0.0086 (6)	0.0071 (6)	0.0094 (6)	-0.0008 (5)	-0.0010 (5)	-0.0014 (5)
C7	0.0100 (6)	0.0122 (7)	0.0130 (6)	0.0000 (5)	-0.0003 (5)	-0.0034 (5)
C8	0.0090 (6)	0.0128 (7)	0.0126 (6)	0.0013 (5)	-0.0012 (5)	-0.0009 (5)
Te3	0.00845 (4)	0.00910 (4)	0.00846 (4)	0.00204 (3)	0.00024 (3)	0.00044 (3)
Te4	0.00689 (4)	0.00985 (4)	0.00835 (4)	-0.00251 (3)	-0.00212 (3)	0.00166 (3)
N5	0.0080 (5)	0.0141 (6)	0.0107 (5)	-0.0020 (5)	0.0006 (4)	-0.0018 (5)
N6	0.0103 (6)	0.0087 (6)	0.0089 (5)	-0.0019 (5)	-0.0009 (4)	0.0003 (4)
N7	0.0099 (6)	0.0096 (6)	0.0083 (5)	-0.0003 (5)	-0.0007 (4)	-0.0009 (4)
N8	0.0082 (6)	0.0145 (7)	0.0113 (6)	-0.0006 (5)	0.0000 (4)	-0.0011 (5)
C9	0.0078 (6)	0.0099 (6)	0.0080 (5)	-0.0007 (5)	-0.0003 (4)	-0.0008 (5)
C10	0.0081 (6)	0.0089 (6)	0.0081 (5)	-0.0019 (5)	-0.0005 (5)	-0.0004 (5)
C11	0.0126 (7)	0.0110 (7)	0.0099 (6)	-0.0042 (6)	0.0010 (5)	0.0001 (5)
C12	0.0099 (6)	0.0139 (7)	0.0127 (6)	-0.0042 (6)	0.0006 (5)	-0.0015 (6)
C13	0.0088 (6)	0.0082 (6)	0.0082 (5)	-0.0008 (5)	-0.0001 (5)	-0.0006 (5)
C14	0.0077 (6)	0.0089 (6)	0.0094 (6)	-0.0018 (5)	-0.0007 (5)	0.0001 (5)

C15	0.0097 (7)	0.0182 (8)	0.0112 (6)	0.0002 (6)	0.0017 (5)	-0.0019 (6)
C16	0.0109 (7)	0.0130 (7)	0.0090 (6)	-0.0010 (5)	-0.0001 (5)	-0.0011 (5)
Te5	0.00776 (4)	0.01048 (5)	0.00853 (4)	-0.00312 (3)	-0.00108 (3)	0.00122 (3)
Te6	0.00945 (4)	0.00712 (4)	0.00926 (4)	-0.00022 (3)	-0.00264 (3)	-0.00145 (3)
N9	0.0172 (7)	0.0121 (7)	0.0120 (6)	-0.0066 (5)	-0.0009 (5)	-0.0015 (5)
N10	0.0157 (7)	0.0108 (6)	0.0091 (5)	-0.0012 (5)	-0.0026 (5)	-0.0022 (5)
N11	0.0072 (5)	0.0115 (6)	0.0106 (5)	0.0000 (5)	-0.0007 (4)	-0.0004 (5)
N12	0.0103 (6)	0.0116 (6)	0.0103 (5)	-0.0034 (5)	-0.0002 (4)	-0.0023 (5)
C17	0.0091 (6)	0.0108 (7)	0.0086 (6)	-0.0028 (5)	-0.0009 (5)	-0.0008 (5)
C18	0.0097 (6)	0.0090 (6)	0.0091 (6)	-0.0013 (5)	-0.0011 (5)	-0.0019 (5)
C19	0.0207 (8)	0.0139 (8)	0.0096 (6)	-0.0043 (6)	-0.0030 (6)	-0.0028 (6)
C20	0.0216 (9)	0.0142 (8)	0.0133 (7)	-0.0083 (7)	-0.0019 (6)	-0.0040 (6)
C21	0.0067 (6)	0.0098 (6)	0.0086 (6)	-0.0010 (5)	-0.0006 (4)	-0.0010 (5)
C22	0.0086 (6)	0.0087 (6)	0.0082 (6)	-0.0009 (5)	-0.0011 (5)	-0.0020 (5)
C23	0.0090 (6)	0.0140 (7)	0.0130 (6)	-0.0036 (5)	-0.0003 (5)	-0.0029 (6)
C24	0.0072 (6)	0.0144 (7)	0.0124 (6)	-0.0005 (5)	-0.0011 (5)	-0.0016 (5)

Geometric parameters (\AA , $^{\circ}$)

Te1—C5	2.1185 (17)	N8—C15	1.341 (2)
Te1—C1	2.1301 (17)	N8—C14	1.345 (2)
Te2—C2	2.1237 (17)	C9—C10	1.405 (2)
Te2—C6	2.1381 (17)	C11—C12	1.388 (3)
N1—C4	1.336 (3)	C11—H11	0.9500
N1—C1	1.342 (2)	C12—H12	0.9500
N2—C2	1.337 (2)	C13—C14	1.405 (2)
N2—C3	1.338 (2)	C15—C16	1.383 (3)
N3—C8	1.337 (2)	C15—H15	0.9500
N3—C5	1.338 (2)	C16—H16	0.9500
N4—C7	1.339 (2)	Te5—C21	2.1105 (16)
N4—C6	1.345 (2)	Te5—C17	2.1332 (16)
C1—C2	1.406 (2)	Te6—C18	2.1209 (17)
C3—C4	1.392 (3)	Te6—C22	2.1281 (17)
C3—H3	0.9500	N9—C17	1.337 (2)
C4—H4	0.9500	N9—C20	1.337 (3)
C5—C6	1.410 (2)	N10—C19	1.336 (2)
C7—C8	1.392 (3)	N10—C18	1.338 (2)
C7—H7	0.9500	N11—C21	1.334 (2)
C8—H8	0.9500	N11—C24	1.335 (2)
Te3—C13	2.1211 (17)	N12—C23	1.338 (2)
Te3—C9	2.1248 (17)	N12—C22	1.339 (2)
Te4—C10	2.1180 (16)	C17—C18	1.409 (2)
Te4—C14	2.1302 (16)	C19—C20	1.386 (3)
N5—C9	1.338 (2)	C19—H19	0.9500
N5—C12	1.340 (2)	C20—H20	0.9500
N6—C11	1.337 (2)	C21—C22	1.408 (2)
N6—C10	1.339 (2)	C23—C24	1.386 (3)
N7—C16	1.334 (2)	C23—H23	0.9500

N7—C13	1.340 (2)	C24—H24	0.9500
C5—Te1—C1	92.54 (6)	N5—C12—C11	121.60 (16)
C2—Te2—C6	91.48 (6)	N5—C12—H12	119.2
C4—N1—C1	117.64 (16)	C11—C12—H12	119.2
C2—N2—C3	117.78 (15)	N7—C13—C14	121.05 (15)
C8—N3—C5	117.52 (15)	N7—C13—Te3	116.77 (12)
C7—N4—C6	117.69 (15)	C14—C13—Te3	122.17 (12)
N1—C1—C2	120.90 (16)	N8—C14—C13	121.25 (15)
N1—C1—Te1	113.35 (12)	N8—C14—Te4	113.13 (12)
C2—C1—Te1	125.74 (13)	C13—C14—Te4	125.59 (12)
N2—C2—C1	120.98 (16)	N8—C15—C16	121.90 (16)
N2—C2—Te2	117.13 (12)	N8—C15—H15	119.0
C1—C2—Te2	121.87 (12)	C16—C15—H15	119.0
N2—C3—C4	121.26 (17)	N7—C16—C15	121.76 (16)
N2—C3—H3	119.4	N7—C16—H16	119.1
C4—C3—H3	119.4	C15—C16—H16	119.1
N1—C4—C3	121.43 (17)	C21—Te5—C17	93.44 (6)
N1—C4—H4	119.3	C18—Te6—C22	93.72 (6)
C3—C4—H4	119.3	C17—N9—C20	117.07 (16)
N3—C5—C6	120.83 (15)	C19—N10—C18	117.32 (16)
N3—C5—Te1	116.33 (12)	C21—N11—C24	117.52 (16)
C6—C5—Te1	122.70 (12)	C23—N12—C22	117.19 (16)
N4—C6—C5	120.95 (15)	N9—C17—C18	121.22 (15)
N4—C6—Te2	114.60 (12)	N9—C17—Te5	113.16 (12)
C5—C6—Te2	124.45 (12)	C18—C17—Te5	125.57 (12)
N4—C7—C8	120.88 (16)	N10—C18—C17	120.98 (15)
N4—C7—H7	119.6	N10—C18—Te6	116.55 (12)
C8—C7—H7	119.6	C17—C18—Te6	122.48 (12)
N3—C8—C7	121.98 (17)	N10—C19—C20	121.55 (17)
N3—C8—H8	119.0	N10—C19—H19	119.2
C7—C8—H8	119.0	C20—C19—H19	119.2
C13—Te3—C9	93.30 (6)	N9—C20—C19	121.84 (17)
C10—Te4—C14	93.80 (6)	N9—C20—H20	119.1
C9—N5—C12	117.13 (16)	C19—C20—H20	119.1
C11—N6—C10	117.26 (15)	N11—C21—C22	121.09 (15)
C16—N7—C13	117.26 (15)	N11—C21—Te5	115.58 (12)
C15—N8—C14	116.70 (16)	C22—C21—Te5	123.27 (12)
N5—C9—C10	121.28 (16)	N12—C22—C21	120.99 (15)
N5—C9—Te3	113.77 (12)	N12—C22—Te6	113.90 (12)
C10—C9—Te3	124.94 (12)	C21—C22—Te6	125.11 (12)
N6—C10—C9	121.09 (15)	N12—C23—C24	121.65 (16)
N6—C10—Te4	115.90 (12)	N12—C23—H23	119.2
C9—C10—Te4	122.91 (12)	C24—C23—H23	119.2
N6—C11—C12	121.62 (16)	N11—C24—C23	121.50 (16)
N6—C11—H11	119.2	N11—C24—H24	119.3
C12—C11—H11	119.2	C23—C24—H24	119.3

C4—N1—C1—C2	0.5 (3)	C16—N7—C13—C14	-1.8 (2)
C4—N1—C1—Te1	-179.04 (14)	C16—N7—C13—Te3	178.54 (13)
C3—N2—C2—C1	-0.8 (3)	C15—N8—C14—C13	-1.2 (3)
C3—N2—C2—Te2	-179.06 (13)	C15—N8—C14—Te4	-179.44 (14)
N1—C1—C2—N2	0.2 (3)	N7—C13—C14—N8	2.9 (3)
Te1—C1—C2—N2	179.73 (13)	Te3—C13—C14—N8	-177.51 (13)
N1—C1—C2—Te2	178.42 (13)	N7—C13—C14—Te4	-179.14 (12)
Te1—C1—C2—Te2	-2.1 (2)	Te3—C13—C14—Te4	0.5 (2)
C2—N2—C3—C4	0.6 (3)	C14—N8—C15—C16	-1.3 (3)
C1—N1—C4—C3	-0.7 (3)	C13—N7—C16—C15	-0.7 (3)
N2—C3—C4—N1	0.2 (3)	N8—C15—C16—N7	2.3 (3)
C8—N3—C5—C6	1.3 (2)	C20—N9—C17—C18	1.5 (3)
C8—N3—C5—Te1	-174.55 (13)	C20—N9—C17—Te5	-176.06 (14)
C7—N4—C6—C5	2.7 (2)	C19—N10—C18—C17	-0.2 (3)
C7—N4—C6—Te2	-177.44 (13)	C19—N10—C18—Te6	179.91 (14)
N3—C5—C6—N4	-3.9 (3)	N9—C17—C18—N10	-1.2 (3)
Te1—C5—C6—N4	171.65 (12)	Te5—C17—C18—N10	176.06 (13)
N3—C5—C6—Te2	176.25 (12)	N9—C17—C18—Te6	178.68 (13)
Te1—C5—C6—Te2	-8.2 (2)	Te5—C17—C18—Te6	-4.1 (2)
C6—N4—C7—C8	0.8 (3)	C18—N10—C19—C20	1.2 (3)
C5—N3—C8—C7	2.3 (3)	C17—N9—C20—C19	-0.5 (3)
N4—C7—C8—N3	-3.5 (3)	N10—C19—C20—N9	-0.9 (3)
C12—N5—C9—C10	-0.8 (2)	C24—N11—C21—C22	2.7 (2)
C12—N5—C9—Te3	178.70 (13)	C24—N11—C21—Te5	-174.54 (13)
C11—N6—C10—C9	1.4 (2)	C23—N12—C22—C21	-1.2 (2)
C11—N6—C10—Te4	-175.06 (12)	C23—N12—C22—Te6	178.49 (12)
N5—C9—C10—N6	-0.5 (3)	N11—C21—C22—N12	-1.3 (2)
Te3—C9—C10—N6	-179.93 (12)	Te5—C21—C22—N12	175.69 (12)
N5—C9—C10—Te4	175.68 (12)	N11—C21—C22—Te6	179.06 (12)
Te3—C9—C10—Te4	-3.8 (2)	Te5—C21—C22—Te6	-3.9 (2)
C10—N6—C11—C12	-1.0 (3)	C22—N12—C23—C24	2.2 (3)
C9—N5—C12—C11	1.2 (3)	C21—N11—C24—C23	-1.7 (3)
N6—C11—C12—N5	-0.3 (3)	N12—C23—C24—N11	-0.8 (3)